# Surface-bulk hybrid mode in 36°-rotated *YX* cut of lithium tantalate with periodic metal grating

N. F. Naumenko[a)]
*Moscow Steel and Alloys Institute, Leninski pr. 4, 117936, Moscow, Russia*

B. P. Abbott
*Sawtek Inc., 1818 South Hwy 441, Apopka, Florida 32703*

(Received 16 July 2001; accepted for publication 19 January 2002)

We report on a surface-bulk hybrid acoustic mode, which exists within a limited frequency interval in some piezoelectric substrates within a periodic metal grating. These hybrid modes result from the coupling between a bulk wave and a counter-propagating surface (or leaky) wave. An example of such a hybrid mode, which propagates in 36°-*YX* cut of lithium tantalate, is described. The hybrid mode gives rise to an additional branch of dispersion relation. The Bragg reflection stop band occurs due to phase match between surface and bulk waves. The lower edge of this stop band manifests itself by a resonance of harmonic admittance, being a reason of undesired resonances in resonator filters. © *2002 American Institute of Physics*. [DOI: 10.1063/1.1459621]

An important requirement of surface acoustic wave (SAW) filters for high frequency applications is low insertion loss, which is provided by using resonator structures on piezoelectric substrates with strong piezoelectric coupling. Leaky surface acoustic waves (LSAW), which propagate along the *X* axis in rotated *Y* cuts of lithium niobate and lithium tantalate (LT), are known to have much higher electromechanical coupling coefficients than that of common SAW. Therefore, these waves are widely used in high-frequency SAW devices. Rotated *Y* cuts of LT with rotation angles from 36° to 42° are especially popular, due to high electromechanical coupling and moderate values of temperature coefficient of frequency. Though LSAWs exhibit non-zero propagation loss caused by bulk acoustic wave (BAW) radiation, with the proper choice of rotation angle and electrode thickness in the grating, this loss can be minimized. Propagation velocity of LSAWs within a grating also depends on the orientation and electrode thickness. As the metal thickness is reduced and the rotation angle approaches 37°, the maximum value of the propagation velocity for the LSAW on LT tends to that of the fast shear BAW. In the absence of the piezoelectric effect and mechanical load caused by the grating, the fast shear BAW, propagating in 37°-*YX* cut, is pure horizontally polarized and leaves the boundary surface free of traction, thus being an "exceptional" bulk wave.[1] Therefore, in orientations close to 37°*YX* cut, within a grating, the bulk wave interacts strongly with the LSAW. This interaction results in parasitic resonances, which degrade SAW filter performance.

The interaction between LSAW and fast shear BAW, propagating in 36°*YX* cut of LT, was recently investigated using numerical techniques. In particular, the method of harmonic admittance (HA) of a periodic grating with sufficiently thick electrodes shows the presence of unexpected resonances. These resonances do not correspond to the LSAW, and are attributed to an additional acoustic mode with propagation velocity slightly smaller than that of the fast shear BAW.[2] In this article, we report the results of studying this mode, and offer an explanation for its presence within the periodic grating.

To understand the nature of the additional mode found in 36°*YX* cut of LT, we first carefully examined the HA function, $Y$, of an infinite periodic grating, versus frequency, $f$, and the normalized excitation wave number, $s=p/\Lambda$, where $p$ is the grating period and $\Lambda$ is the wavelength (period) of harmonic excitation. The concept of harmonic admittance was introduced by Blotekjaer[3,4] and further developed[5,6] for simulation of resonator SAW filters and extraction of surface wave characteristics. The HA function represents the admittance of an individual electrode in a periodic array of electrodes and relates electric current $I_n$ on the electrode to the applied harmonic voltage $V_n$:

$$I_n = V_n Y(f,s), \tag{1}$$

where

$$V_n = V_T \exp(j2\pi ns)\exp(j2\pi f). \tag{2}$$

Figure 1 shows harmonic admittance as a function of the ratio $s$, at different values of frequency in the vicinity of the upper edge of the LSAW stop band. Calculations were performed for short-circuited aluminum grating with electrode width to periodicity ratio $\mu=0.5$ and normalized electrode thickness $h/\Lambda=0.04$. A numerical technique, which combines matrix formalism for finding discrete Green functions with the finite-element method used for analysis of electrode structure,[7,8] was utilized to calculate harmonic admittance and velocity dispersion in the grating. We used a normalized frequency, $f'=fp/V_{\mathrm{BAW}}$, where $V_{\mathrm{BAW}}$ is the velocity of the fast shear BAW.

When $f'=0.497$, there are two resonances of $\mathrm{Im}(Y)$, at $s_1=f'$ and $s_2=1-f'$, labeled with numbers 1 and 2 in Fig. 1. Resonance 2 is an image of resonance 1 and a necessary

a)Electronic mail: nnaumenko@ieee.org

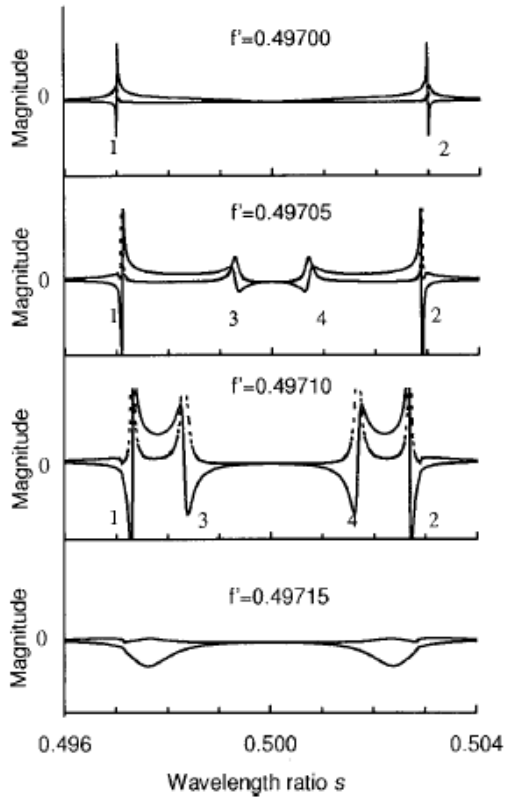


FIG. 1. Harmonic admittance $Y$ as function of the ratio $p/\Lambda$, for leaky wave propagating in 36°$YX$ cut of lithium tantalate with short-circuited aluminum grating. Normalized frequency $f'=fp/V_{\mathrm{BAW}}$ is fixed for each plot. Dashed and solid lines indicate real and imaginary parts of $Y$, respectively.

result of the discrete nature of the electrodes' electrical excitation, Eq. (1), which displays symmetry with respect to $s=0.5$. Hence, $s_{1,2}=0.5\pm(f'-0.5)$. Each resonance represents an acoustic mode in the grating. Its velocity $V$ can be inferred from the mode's resonance frequency, $f_{\mathrm{RES}}$, and spectral frequency, $s_{\mathrm{RES}}$, as $V=V_{\mathrm{BAW}}f'_{\mathrm{RES}}/s_{\mathrm{RES}}$, provided that the propagation loss, determined by $\mathrm{Re}(Y)$, is negligible. Thus, at $f'=0.497$, the velocities of two modes associated with resonances 1 and 2, are $V_1=V_{\mathrm{BAW}}$ and $V_2=V_{\mathrm{BAW}}(1-s_2)/s_2$, respectively. If the periodicity of HA is taken into account, $Y(1-s)=Y(-s)$, it is obvious that resonances 1 and 2 refer to the counter-propagating BAW modes. The backward propagating mode (resonance 2) is characterized by the negative value of derivative $\partial[\mathrm{Im}(Y)^{-1}]/\partial s$ estimated at the pole, $[\mathrm{Im}(Y)]^{-1}=0$. As the normalized frequency is increased from 0.497 00 to 0.497 05 and 0.497 10, resonances 1 and 2 move slowly from $s_{\mathrm{RES}}=0.5\pm(f'-0.5)$ towards $s_{\mathrm{RES}}=0.5$. This implies that the counter-propagating acoustic modes, which correspond to these resonances, have propagation velocity just slighting less than the fast shear bulk mode.

In the same frequency interval, an additional resonance, 3, and its image, 4, appear at $s_3=s_4=0.5$ and move slowly towards resonances 1 and 2, respectively. Resonances 3 and 4 are produced by LSAW mode. The reflection of this mode in the grating results in the Bragg stop band. Due to the symmetry of the crystal orientation, the maximum resonance of HA is produced by LSAW mode at the lower edge of the

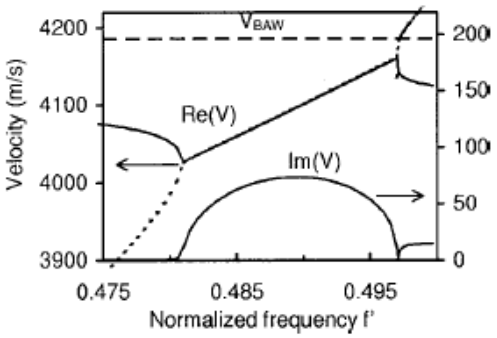


FIG. 2. Velocity dispersion of LSAW (real and imaginary parts) in 36°$YX$ cut of lithium tantalate with short-circuited aluminum grating.

stop band, $f'=0.481$, while no resonance occurs at its upper edge, $f'=0.497$. As the normalized frequency is increased from 0.497 00 to 0.497 05 and 0.497 10, resonances 3 and 4 diverge in Fig. 1 and their amplitudes grow. Finally, at $f'\approx 0.497\,12$, resonances 3 and 4 merge with resonances 1 and 2, respectively. The resulting maximum of harmonic admittance decays rapidly with further increasing frequency, thus showing the decrease of acoustic power radiated by the grating. According to the sign of $\partial[\mathrm{Im}(Y)^{-1}]/\partial s$ at the pole, resonance 3 corresponds to the backward propagating LSAW. Thus, at $f'\approx 0.497\,12$, the interaction occurs between the counter-propagating LSAW and BAW modes.

All analyzed modes are confined in the velocity interval ($V_{\text{max-LSAW}}$, $V_{\mathrm{BAW}}$), where $V_{\text{max-LSAW}}$ is the maximum LSAW velocity in the short-circuited grating. To verify the existence of these four modes, the rigorous numerical solution of the dispersion relation has been performed for 36°$YX$ cut of LT and the results are shown in Fig. 2. The main branch of the dispersion curve (solid line) refers to the forward propagating mode in the grating. It is characterized by the normalized wave number ratio $s_+$ and exhibits the stop band between the frequencies $f'=0.481$ and $f'=0.497$, due to the phase match between LSAW space harmonics with wave numbers $k_0$ and $(k_0-2\pi/p)$, with a small admixture of other space harmonics. In the stop band, $\mathrm{Im}(V)$ grows indicating that there is a standing wave, with no acoustic energy radiated in forward or backward directions. Another branch of dispersion curve shown in Fig. 2 (dotted line) refers to the backward propagating LSAW mode in the grating, with the normalized wave number ratio $s_-=1-s_+$. This mode is symmetric with respect to the forward LSAW mode.

As shown in Fig. 3, at normalized frequencies $f'>0.497$, the backward LSAW mode interacts with the forward BAW. The numerical results presented in Fig. 3 are consistent with the behavior of harmonic admittance in Fig. 1 and can be interpreted in the following way. The backward propagating LSAW mode traps the energy of the forward propagating BAW and gives rise to a mode, which can be referred to as the "SAW/BAW hybrid mode" (SBH). It exists in a narrow frequency interval and decomposes into pure BAW and counter propagating LSAW outside this interval. In analogous way, the forward LSAW mode propagating in the grating interacts with the backward propagating BAW mode. Hence, the dispersion relation has four solutions in the

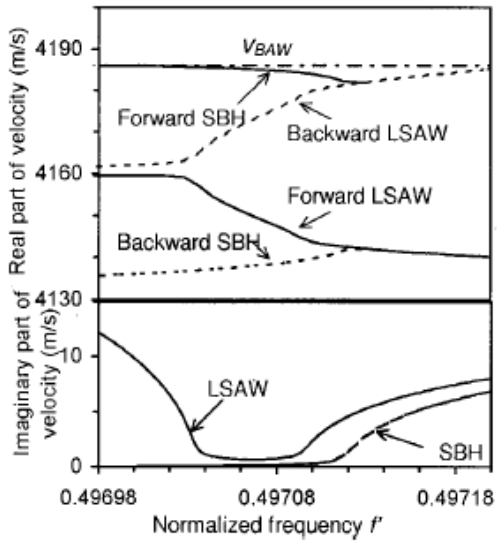


FIG. 3. Enlarged fragment of Fig. 2 showing velocities (real and imaginary parts) of two LSAW and two SBH, which exist in the interval of normalized frequencies $f_p/V_{BAW}$ from 0.496 98 to 0.497 20.

analyzed frequency interval, two LSAW modes (forward and backward) and two SBH modes (forward and backward).

Merging of the BAW with counter-propagating LSAW at $f' \approx 0.497\,12$ can be interpreted as the lower edge of the stop band composed by these modes. It agrees with the behavior of $\mathrm{Im}(V)$, which grows beginning from this frequency, due to the Bragg reflection condition fulfilled. Thus, the lower edge of the SBH stop band can be considered as the cutoff frequency of the bulk wave radiation. In the absence of SBH mode, the cut-off frequency would be higher and determined as an intersection between the velocities of BAW and counter-propagating LSAW. Analysis of derivative $\partial[\mathrm{Im}(Y)^{-1}]/\partial s$, which indicates the power transfer from electric source to radiated acoustic waves in the grating,[4] has shown that maximum resonance due to generation of the SBH mode is expected at the frequency $f' = 0.497\,12$, that is at the lower edge of the SBH stop band.

In addition to this example, we have found the branches of dispersion curves, which can be identified as SBH modes, in some other crystals and orientations, close to that in which one of surface skimming BAW is exceptional. With deviation from such orientation, the SBH mode eventually disappears. The SBH mode can be pure SAW, LSAW, or high-velocity LSAW, dependent on whether the generating exceptional BAW is slow quasishear, fast quasishear or quasilongitudinal. The behavior of the SBH mode also depends on whether its stop band overlaps with the LSAW stop band or not and obviously requires rigorous analytical treatment.

In conclusion, we have reported the example of a surface-bulk hybrid acoustic mode, which occurs within a limited frequency interval in some piezoelectric substrates with a periodic metal grating, due to the coupling between a bulk wave and a counter-propagating surface or leaky wave. Such modes can be a reason of undesired resonances in resonator SAW filters. However, these resonances can be reduced by the proper choice of substrate orientation.

[1] N. F. Naumenko, J. Appl. Phys. **79**, 8936 (1996).
[2] Y. Fusero, S. Ballandras, J. Desbois, J. M. Hode, and P. Ventura, *Proceedings of the 2000 IEEE Ultrasonics Symposium, San Juan* (IEEE, New York, 2000), pp. 163–166.
[3] K. Blotekjaer, K. A. Ingebrigtsen, and H. Skeie, IEEE Trans. Electron Devices **20**, 1133 (1973).
[4] K. Blotekjaer, K. A. Ingebrigtsen, and H. Skeie, IEEE Trans. Electron Devices **20**, 1139 (1973).
[5] Y. Zhang, J. Desbois, and L. Boyer, IEEE Trans. Sonics Ultrason. **40**, 183 (1993).
[6] P. Ventura, J. M. Hode, M. Solal, J. Desbois, and J. Ribbe, *Proceedings of the 1998 IEEE Ultrasonics Symposium, Sendai* (IEEE, New York, 1998), pp. 175–186.
[7] G. Endoh, K. Hashimoto, and M. Yamaguchi, Jpn. J. Appl. Phys., Part 1 **34**, 2638 (1995).
[8] E. L. Adler, IEEE Trans. Ultrason. Ferroelectr. Freq. Control **41**, 876 (1994).